A SELF RECONFIGURABLE UNDULATING GRASPER FOR ASTEROID MINING

Suzanna Lucarotti[1], Chakravarthini M Saaj[1], Elie Allouis[2] and Paolo Bianco[3]

[1]*Surrey Space Centre, Guildford UK* [2]*Airbus DS, Stevenage UK* [3]*Airbus, Portsmouth UK*

ABSTRACT

Recent missions to asteroids have shown that many have rubble surfaces, which current extra-terrestrial mining techniques are unsuited for. This paper discusses modelling work for autonomous mining on small solar system bodies, such as Asteroids. A novel concept of a modular robot system capable of the helical caging and grasping of surface rocks is presented. The kinematics and coordinate systems of the Self RecoNfigurable Undulating Grasper (SNUG) are derived with a new mathematical formulation. This approach exploits rotational symmetry and homogeneity to form a cage to safely grasp a target of uncertain properties. A simple model for grasping is evaluated to assess the grasping capabilities of such a robot. The results presented show the utility of this formulation.

Keywords: modular robot, asteroid mining, space robotics, reconfiguration.

1. INTRODUCTION

In-Situ Resource Utilisation (ISRU) remains a key disruptive technology to enable cost-effective long term exploration and exploitation of the Solar System [1]. A key enabling feature for this is mining raw materials off-Earth, but previous research has focussed on low gravity regolith mining, primarily on the Moon [2, 3]. This kind of mining is suitable for very large asteroids and minor planets and above, and relies on lower gravity Earth analogue methods to manipulate fine regolith. It is relatively easy to test terrestrially with lunar simulants [4], with the current leading robot being the NASA RASSOR project [5]. Lunar mining is being developed for Lunar bases and capital intensive Deep ISRU is the preferred approach[6]. Since the Moon is within range of teleoperation from Earth and possible crewed missions, fully autonomous robotic mining is not critical.

Asteroids and Comets are members of the International Astronomical Union defined class of Small Solar System Bodies (SSSBs) [7]. They are very small with very low gravity, and the largest asteroid (Ceres) is not an SSSB, but rather a dwarf planet. There are numerous SSSBs - as of April 2019, almost 20,000 Near Earth Asteroids (NEAs) alone have been discovered [8]. Of these, 897 are estimated as over 1km diameter and 4133 as 300-1000m diameter. While surface features remain mostly unknown, mass and orbit parameters are available. The closest NEAs can be reached with less ΔV than the Moon.

There have been so far been five missions to the surface of SSSBs - NEAR-Shoemaker to Eros, where they unexpectedly landed [9], Hayabusa 1 to Itokawa [10], Rosetta to the Comet 67P Churyumov-Gerasimenko [11], Hayabusa 2 to Ryugu [12], and OSIRIS-Rex to Bennu [13]. Hayabusa 2 and OSIRUS-Rex are both currently live missions. Detailed close-range surface images have been obtained from Itokawa, 67P and Ryugu, higher altitude images from low orbit or prior to landing have been received from the others.

An unexpected recent result from surface operations on SSSBs has been the prevalence of rubble pile asteroids. [14, 15]. Astronomical thermal inertia models of Bennu were believed to suggest small grain sizes for surface material [16] when in fact Bennu appears to be a rubble pile with many macroscopic rocks. Rubble pile dynamics are an active research subject, with various mechanisms proposed to explain their apparent gardening and unexpectedly cohesive structure, for a discussion see [17].

Existing extraterrestrial sampling techniques rely upon collecting fine dust for processing or sample return. Typically with a penetrator or compressed gas to force dust up into a horn, or a contact trap [12, 18]. Current surface sample return techniques require mission planners to find a large landing ellipse containing no large boulders to allow the spacecraft to approach the surface without risk of collision. Sampling on Ryugu was delayed due to the unexpected sparsity of safe sampling areas [19].

The surface of Ryugu has been now imaged closeup with the Minerva I and II landers (Fig. 1). The relative sparsity of regolith and preponderance of rocks makes a mining approach based solely on collecting regolith challenging, as piles of rocks must be searched or pulverised in-situ to obtain it. The other potential approach is to work with the rocks. This is a difficult challenge as it requires grasping unknown targets in a cluttered and potentially unstable environment. The only known research similar to this concept with asteroids was part of the studies for the now discontinued NASA Asteroid Redirect Mission [20], where the preferred mission approach was for the spacecraft to secure a 2-4m boulder from the surface and

return it to cislunar space for human inspection.

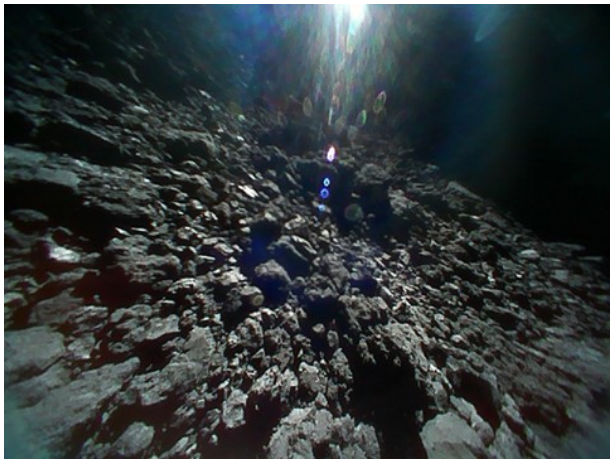

Figure 1. Surface of Ryugu © JAXA

There are numerous challenges involved in mining on a small SSSB are many. Wheeled locomotion is impossible due to tiny surface escape velocity, any force applied must be carefully metered and modelled to avoid accidentally launching the miner into Space. Gravity is not sufficient to anchor spacecraft to the body, and simply moving internal masses may cause spacecraft motion (the Minerva landers on Ryugu exploit this to bounce around the surface). Mining on SSSBs is more akin to on-orbit construction than conventional mining; to mine a rubble pile structure, one or more rocks must be grasped, manipulated and then moved to a defined repository where further processing can then occur. It must be able to carry this out autonomously and reliably without direct human supervision.

Robotic manipulators used in Space fall into a number of categories (see Tab. 1). To collect samples or mine the surface, a manipulator that can safely and reliably handle a natural target object based on only an estimate of its shape, mass and surface properties is required. This requirement rules out pallet grippers, electrostatic, magnetic and ingressive grippers. This leaves methods that achieve either a form closure or force (frictional) grasp. A net or bag style gripper, while demonstrated in Space [21] and providing form closure, is hard to control in a cluttered environment such as the top of a rubble pile. Further, the refolding [22] and recovery requirements (assuming it is tethered, current space nets have not been) make autonomous reusability challenging. This leaves fingered hands as the only current viable technology. These, unless they encircle the target prior to contact, must be extremely precise with contact points and forces to avoid accidentally pushing the target away during force transfer.

Prior encircling or caging of a target is a promising topological and geometric concept to address uncertainty in grasping [23]. It formulates finger positions that restrict an object's position within a given area or volume, linear motion of the target is bounded before contact is made, preventing serious touch rebound effects. The cage can then be converted into a form closure or force grasp [24].

Modular and reconfigurable robots have been proposed for Space, and many protoypes have been tested on the ground, thus far the research focus has been on locomotion methods [25] or agent based techniques. Robot arm dynamics under gravity means that base joints must be sized to support the weight of the entire arm and so tend to taper to the end effector. The computational complexities of conventional inverse kinematics (IK) keep most conventional arms close to 6 Degrees of Freedom (DoF) as analytical IK solutions are available [26].

Rest of this paper is organised as follows: Section 2 presents the novel concept of SNUG that is designed to operate in microgravity conditions. Section 3 presents the kinematics formulation and co-ordinate frames for path and grasp planning and sizing. Section 4 implements these formulae with a simple theoretical model and assesses the capabilities of such a robot. Finally, concluding remarks and direction for future research is stated in Section 5.

2. THE SNUG CONCEPT

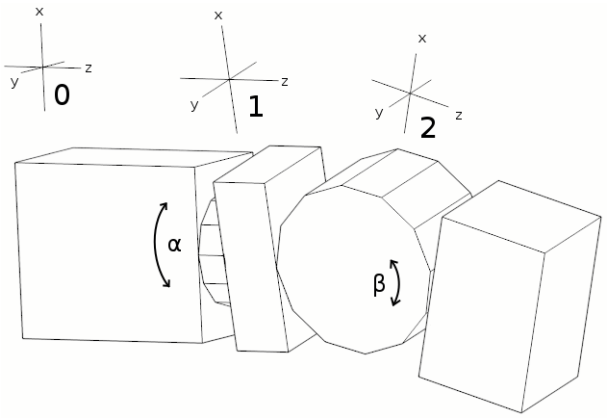

Figure 2. Coordinate frames by section across a SNUG module

The Self recoNfigurable Undulating Grasper (SNUG) concept is presented here to address microgravity manipulation on SSSBs. This is a novel modular robot consisting of a chain of identical, interchangeable, rigid but articulated modules (see Fig. 2), each with two androgynous mating points at either end which can connect to other modules. These connection points will enable the transmission of mechanical forces and power (data either directly or through a wireless link). Each module will have two DoF: a hinged joint and a twisting joint, enabling each module a wide field of movement similar to a human wrist. The surface of each module will be a rigid material capable of maintaining consistent physical properties in a Space environment with extreme temperature changes. All actuation shall be local to the module (no tendons). Repeatedly using the same joint values across

Table 1. Review of current grippers for Space

Gripper	Description	Comments
Two-finger	Items are held between fingers pushing together or apart to maintain grip	Small contact area ensures a larger force must be utilised to ensure sufficient frictional force to maintain a firm grip. Precise control required, little tolerance of positioning inaccuracies.
Multi-finger	A claw like structure that grasps the target by partially encircling it.	Flown in Space with Robonaut and the Robonaut2 hand on the ISS. Highly complex, designed for teleoperation [27].
Pallet	Adaptor designed to mate with standard attachment points	Most successful current space technology e.g. Latching End Effectors on SSRMS [27].
Octopus	Flexible surface encircles target and grips with friction	Flexible material properties are typically highly sensitive to temperature. The robot will experience large temperature variations.
Magnetic	Use an electromagnet to grip ferromagnetic materials	Limited to ferromagnetic targets.
Ingressive	Pick up material by extending gripper parts into it (e.g. Harpoon)	Demonstrated successfully on RemoveDEBRIS mission [21].
Electrostatic	Create a charge difference between target and gripper	Limited by Surface Area, typically specialised to gripping planar surfaces [28].
Net	Fire a net at the target and entangle it	Successfully demonstrated with RemoveDEBRIS mission [21]. Requires bullets to deploy from cannister, sensitive to packing.

adjacent modules produces a helical structure capable of wrapping around objects, enabling it to grasp without an end-effector.

This design allows the arm to curl around the target before making contact with its surface. One approach to capture is to use the ground as a base, build walls with the helical structure and close it at the top with the free end as it returns to the robot base station, forming a virtual cage around the target rock. Then, assuming the rock does not break upon tightening, any rebound from initial contact should be contained safely, and a secure grip can be established before any attempt to manipulate the rock. If the rock has a concave surface then the arm can achieve a form closure grasp that should be able to transmit forces in all directions with just an encirclement of more than 180° to grasp the object. All other surfaces can have a loose or tight form closure grasp around them, enabling transport without needing to crush an object with unknown surface properties. The maximum local curvature of the structure would be defined by the joint range of motion, and this defines (with the module dimensions) the sizes that can be picked up in an encircling manner.

The SNUG concept can be understood as a generalised three-dimensional solution to the caging problem, replacing separate contact points in 2D with one encircling space curve. The helical cage forms a partial generalised solution to immobilising any target object, which when combined with environmental or further encirclement to seal the ends, provides a complete solution to immobilise any object thicker than the largest 3D gap size in the structure (this is may be the distance between the bars of the cage, between environment and the cage bars, or between bars in any end cap structure). A pre-grasping cage is also well understood as an intermediate step towards a secure grasp and provides a robust mathematical method to guarantee theoretically that the target object will not escape. This study appears to be the first study of 3D caging using a single finger rather than more anthropomorphic systems.

The reference concept of the SNUG robot is that it is attached to an Asteroid Lander base which has an opening leading to an onboard sample processing unit. The task for the robot then is to collect rocks from the local environment and place them into the sample container for processing. In addition to mining of asteroids, the SNUG concept is also applicable to on-orbit construction, debris capture and potentially terrestrial applications.

The large number of modules makes failure of individual modules more likely. Nonetheless the reconfigurable modular design the robot shows graceful degradation. By attaching both ends to active ports on the base spacecraft, the robot could detach the failed module on one side and attach it to a storage port reattach to the other section, disconnect one end from a port and continue as before with only a small loss in capabilities.

3. KINEMATICS AND GRASP PLANNING

To aid in reliable grasping of unknown targets, a caging approach is used for grasping stationary targets, with the displacement of the target fully bounded prior to making contact with SNUG. It is observed that the SNUG geometry is well suited to forming helical structures and this simplifies the resultant kinematics considerably; the computational complexity scales up with number of helical segments, and not modules.

In Fig. 2-4 & 6, sections of the SNUG modules are represented as cuboids, with approximated cylinders representing joints. The lengths of each section (from joint centre to joint centre or cuboid tip) are critical, but the width and height are not for the purposes of the kinemat-

ics (but do eventually contribute to gap sizes). The SNUG design will have integrated joints and sections, and the width and height are likely to be circular to enable consistent caging sizes; this is not shown here for reasons of clarity, with cuboids more easily showing rotations to the reader. Unless otherwise stated, all drawings are orthographic.

Each module is linked together by two joints, an α joint providing roll control between sections, and a β joint providing pitch or hinge-style control between sections. The modules are numbered from the base and connected together, with the zeroth module assumed to be attached to a base spacecraft. The convention adopted here is that 1the α joint is connected before the β joint, however this is arbitrary and can be reversed with only minor corrections to the formulae presented.

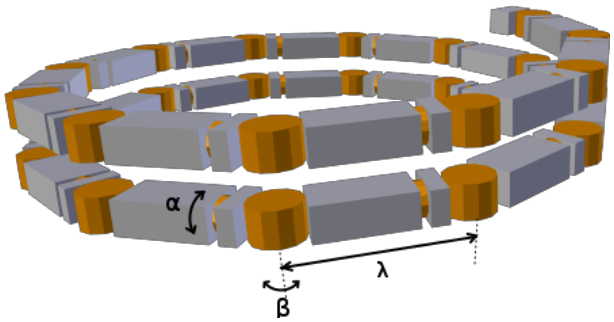

Figure 3. Annotated perspective render of a SNUG Helical cage. Low α and β angles lead to small side gaps and a wide caging cylinder

An assembled series of modules is referred to as a structure or cage (see Fig. 3), and forms a pseudo-helical twisted ladder-like structure, the straight rungs of which shall be referred to as bars, as they form this when used as a caging structure. It should be noted that each bar in fact contains parts of two consecutive modules connected rigidly together. The length of each bar is defined as λ and is also the straight length of each module due to the module homogeneity. ν and η are ratios together expressing the relative section lengths thus: The distance between α and β joints is $\nu\lambda$, the distance between β joint and module end is $\eta\lambda$ and the distance between the α joint and the module start is $(1-\nu-\eta)\lambda$. The resultant structure, as shall be shown derives solely from λ, α and β, which for any given SNUG helical structure are constant throughout. The end to end homogeneous tran1sformation in the module end frame is seen in Eq. 1. In Denavit-Hartenburg co-ordinates, this is equivalent to three transformations as shown in Tab. 2. The following convention for trigonometric functions is observed: $C_\alpha = \cos(\alpha); S_\beta = \sin(\beta)$.

$$\mathbf{A}_2^0 = \begin{bmatrix} C_\alpha C_\beta & -S_\alpha C_\beta & S_\beta & \lambda S_\beta (1-\eta) \\ S_\alpha & C_\alpha & 0 & 0 \\ -C_\alpha S_\beta & S_\alpha S_\beta & C_\beta & \lambda(\eta + (1-\eta) C_\beta) \\ 0 & 0 & 0 & 1 \end{bmatrix} \quad (1)$$

Table 2. Equivalent DH parameters

Stage	twist angle	link length	joint angle	offset distance
1	0	$11-\nu-\eta$	π	0
2	π	0	α	ν
3	-π	η	β	0

If η is set to 1 then the mapping occurs directly from the start of one bar to the start of another. In this way, some of the specifics of the snug geometry lengths can be avoided in the calculations. Here η is applied as a simple translation correction to the final value when transitioning from local module to world coordinates. This results in the simpler $\mathbf{A}_{snug}$ transformation given in Eq. 2.

$$\mathbf{A}_{snug} = \begin{bmatrix} C_\alpha C_\beta & -S_\alpha C_\beta & S_\beta & 0 \\ S_\alpha & C_\alpha & 0 & 0 \\ -C_\alpha S_\beta & S_\alpha S_\beta & C_\beta & \lambda \\ 0 & 0 & 0 & 1 \end{bmatrix} \quad (2)$$

The transformation from base end effector coordinate frame to helical centreline aligned intermediate Eulerian coordinate frame is two rotations, one around the x-axis (θ_x), and one around the z-axis (θ_z), given by $\mathbf{Q}$ (Eq. 3)

$$\mathbf{Q} = \begin{bmatrix} C_z & S_z & 0 & 0 \\ -C_x S_z & -C_x C_z & S_x & 0 \\ S_x S_z & -S_x C_z & C_x & 0 \\ 0 & 0 & 0 & 1 \end{bmatrix}, \quad (3)$$

where $C_x = \cos\theta_x; \quad S_z = \sin\theta_z.$

The two rotation angles are as given in Eq.4,

$$\theta_z = -\alpha/2; \qquad \tan\theta_x = T_b/S_a, \quad (4)$$

with a further convention of $S_a = \sin(\alpha/2)$ and $T_b = \tan(\beta/2)$.

The z-axis is then aligned with the helical centreline, and the cylindrical coordinates are then derived (Eq. 5, 6) for two helices, one with the minimum radius (r_i see Eq. 7) and the maximum radius (r_o see Eq. 8) of the structure.

$$\tan \Delta\theta = \frac{C_a\sqrt{T_b^2 + S_a^2}}{T_b/T_\beta - S_a^2} \tag{5}$$

$$\Delta z = \frac{\lambda S_a}{\sqrt{T_b^2 + S_a^2}} \tag{6}$$

$$r_i = \frac{\lambda C_a C_b}{2\sqrt{(1 + S_a^2/T_b^2)\,(1 - C_a^2 C_b^2)}} \tag{7}$$

$$r_o = \frac{\lambda}{2\sqrt{(1 + S_a^2/T_b^2)\,(1 - C_a^2 C_b^2)}} \tag{8}$$

The positioning of modules then follows a regular helical structure, with a constant Δz and $\Delta\theta$, and constant inner and outer radius, which bound the contact area for caging an object; it also defines the widest cylinder that can be encircled and the narrowest cylinder that can be ingressively grasped. The best case and worse case SNUG section radii must also be added or subtracted from these for assessing contact distances. The use of two helices captures the reality that the structure is not a perfect plane curve, and has bulk and rigid modular sections of varying local radii in a cylindrical frame.

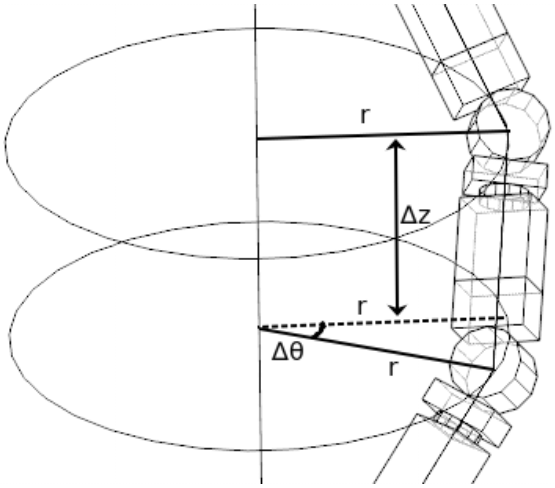

Figure 4. Cylindrical co-ordinates for a SNUG helical cage

The gripping properties can now be assessed with a simple model. The distance between bars is at maximum along the z direction when a full rotation has been accomplished. The gap is reduced by the thickness of the SNUG sections (here modelled to be constant r_{arm}). Treating the structure as a smooth curve rather than a rigid structure, the worst case value for the side gap (assuming the top and bottom of the virtual cylinder are the openings) is given by Eq. 9.

$$g_s = 2\pi\Delta z/\Delta\theta - 2r_{arm} \tag{9}$$

A conservative caging requirement is to encircle it twice to ensure sufficient contact points for all shapes when closing. This requires M_c modules devoted to forming the cage, where $M_c >= 4\pi/\Delta\theta$ [$M_c \subset \mathbb{Z}$]. The length of the caging cylinder is then $M_c\Delta z$. A planar slice through the centreline of a successful cage can be seen in Fig. 5.

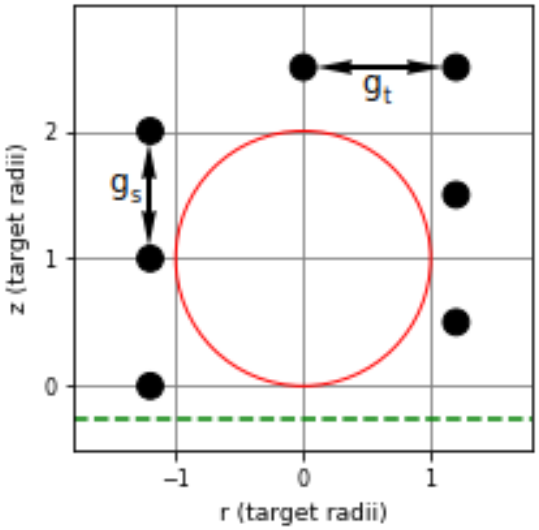

Figure 5. 2D caging view (sliced down centreline) of a successful caging - full closure from the ground at the bottom and the top by the manipulator arm (top centre contact point).

The kinematics of the resultant system are found to be dependent on the number of segments and not the total number of modules as they exploit rotational symmetry. The morphology of the resultant structure can be effectively modelled using regular continuous space curves, which can then be easily converted into joint parameters for the SNUG modules.

4. MODELLING A SIMPLE USE CASE

The snug robot is organised into two structures, a caging cylinder with suitable α and β values to cage the target diameter (with a 20% margin to cover perceptual difficulties and the arc motion of the arm). The cage is sized to encircle the target twice, to ensure any subsequent contact fully encircles it. The cage is then lowered over the target without touching it. The SNUG module cross-section is assumed to be uniformly circular, and of a radius r_{arm}, which also must be accounted for in sizing the caging cylinder.

Target samples are modelled as isolated spheres on a flat surface with a radius r_{targ}. A goal for this model is to assess what can be collected with given SNUG properties. The modelled SNUG robot has 20 modules, module length of 1m and each module section has a constant radius of 0.1m. A rendering of the model can be seen in Fig. 6

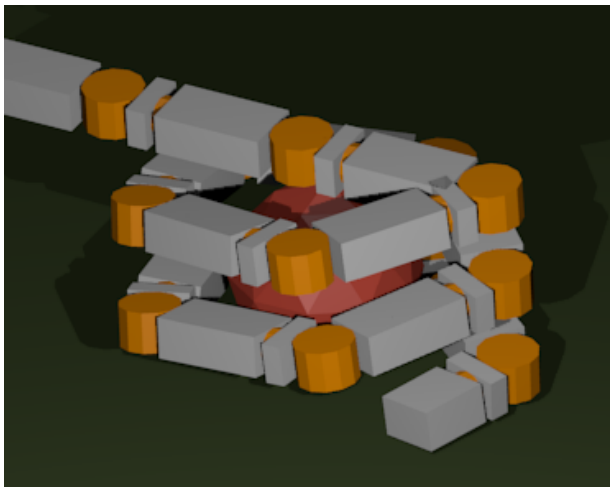

Figure 6. A perspective render of caging with this model

$\therefore M_t = 20; \lambda = 1; r_{arm} = 0.1$

Caging is obtained by finding the most efficient cage that satisfies all constraints identified in Tab.3. Various margins of safety were implemented in the model to demonstrate robust behaviour in an uncertain environment. The unused modules then provide the positioning of the cage, with the constraint that the interface to the cage between segments is on the far side of the cage, partially closing the top of the cage. The cage is then lowered over the target rock. The sphere will then be fully caged, and the cage can then tighten around the target and form a friction or form closure grip before lifting the target and placing it in the spacecraft opening.

The caging cylinder is restricted at the top and manipulated by the other structure, a positioning arm that connects the base spacecraft to the caging cylinder. The top restriction is formed by the positioning arm bisecting the top of the cage as it connects to the far side. This can be simply modelled with g_t as the maximum top gap width (Eq. 10). The unused caging modules form the positioning arm and their number establishes the grasping range of that configuration.

$$g_t = r_i - 2r_{arm} \tag{10}$$

Once the cage is in place over the target the displacement of the target will now result in contact with the ground or cage, trapping the target. The cage can then be tightened to ensure a frictional or form closure grip independent of the ground plane, without risking losing the target during grasping. The positioning segment can then be used to lift the target and place it into the target receptacle on the spacecraft. The kinematics and SNUG configuration thus define the range of target diameters graspable, and the range from a base station that can be grasped without requiring base relocation.

In this intermediate frame, the mapping to cylindrical coordinates has been given previously (Eq. 5 - 7) the inverse is simply a function of finding the bar location and reference frame for the given module in the chain (n) and then moving to the specified site of the end effector. Note that r_i always touches the midpoint of the bar, and the bar is perpendicular to the origin here. It is then rotated by $n\Delta z$ around the z axis to move to helical Eulerian, and transformed by $\mathbf{Q}^T$ to move to a frame centred at the initial end effector as shown in Eq. 11. This is valid across each segment, so computation requirements scale up by segments, rather than modules. In this grasping model, a maximum of three separate items in the kinematic chain are required (the interface segment is not modelled at this stage as it will have minimal effect on grasping capabilities, and is assumed to perfectly combine with the positioning segment).

$$\mathbf{Q}^T \begin{bmatrix} \cos n\Delta\theta & \sin n\Delta\theta & 0 & 0 \\ -\sin n\Delta\theta & \cos n\Delta\theta & 0 & 0 \\ 0 & 0 & 1 & 0 \\ 0 & 0 & 0 & 1 \end{bmatrix} \begin{bmatrix} r_i \\ -\lambda/2 \\ n\Delta z \\ 1 \end{bmatrix} \tag{11}$$

To find an optimal solution in terms of α and β for each target radius, the floating point value of M_c was used as a scoring value and subjected to a minimisation function, with constraint breaking cases given an arbitrarily high value. This found the minimum number of modules required for the cage, freeing up the other modules to form a manipulator arm to reach the target. This can be visualised as a grasping map (see Fig. 7), with possible values of α and β forming a small viable region satisfying all constraints. As per this figure, for 30cm targets, the optimal result is the rightmost point where $\alpha = 7.7°$ and $\beta = 94.0°$. The edges of the region correspond to the constraints - Clockwise from the top left edge, Target radius smaller than side gap, Cage radius too small, Cage length too short and Target radius smaller than top gap (with margins for error).

Table 3. Simulation constraints

Constraint	**Comments**
$r_{targ} < 1.2r_i$	20% margin for cage radius to ensure contactless placing
$2r_{targ} > g_s$	10% margin on target diameter not fitting through side gaps
$2.2r_{targ} > g_t$	10% margin on target diameter not fitting through top gap
$2r_{targ} < 1.1M_c\Delta z$	10% margin on cage deep enough to contain target
$g_s > 0.2r_{arm}$	20% margin on tightly coiling to avoid self-collision
$g_t > 0.2r_{arm}$	20% margin on closing the top to avoid self-collision
$M_c < M_t$	At least one spare module is needed for positioning the cage
$\lambda(M_t - M_c) > 2.2r_o$	20% margin to reach far side of cylinder by positioning segment

Multiple grasping maps were generated for the full range

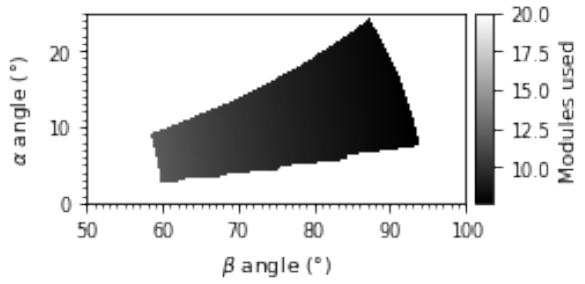

Figure 7. Grasp map for 30cm targets

of manipulable target sizes, with solutions for all constraints found from 20cm up to 1.89m. Across this range α stays between 3° and 7°, suggesting this joint range will not be driven by coiling requirements. β ranges from 133° for the smallest target, to 44° for the largest. This demonstrates similar grasping styles to those found in human hands. Obtuse angles correspond to delicate fingertip manipulation of small objects, where only the finger tips touch it. Acute angles correspond to robust full hand gripping, where the contact area is the inside of the fingers. The smallest manipulable size is defined by the constraints signalling risk of self-collision, and the largest by using all SNUG modules for caging, so that there is no range for manipulating the cage. Arm sizing for SSSB missions will be dependent on repository opening diameter and volume, desired arm range (grasping too close to a base station might undermine local rubble pile stability).

Visualisation of the robot is achieved using custom Blender code. It is noted that by using α values of 180°, linear motion can also be generated as the structure is now a regular zig-zag with β defining the length of the structure. This shows that the repeated α and β formulation supports all necessary range of motion for positioning as well as caging, so could be used to control the positioning segment in addition to the cage.

Fig. 8 shows the optimal grasp cases for each target size with the given SNUG configuration. The steps demonstrate the tradeoff between caging modules and manipulator segments, and the slight slope is a function of the need to use part of the manipulator to form the top of the cylinder. With application to Asteroid mining and known surface features, this configuration can safely manipulate a wide range of targets over a wide area from 20cm up to nearly 2m. The possible mass range assuming typical chondrite density of $3g/cm^3$ is 100kg to 100 tonnes. This substantially reduces risk that surface material will not be graspable by the spacecraft. Once the target items have been securely grasped, less modules will need to be dedicated to the grasping (as this covers the worst case scenarios), and targets can be placed a further distance away from the robot base.

The size range is determined by both the total number of modules and the module length. Larger modules can grip targets down to a fraction of their size, but are less efficient at freeing up the manipulator segment as target size changes than multiple smaller modules.

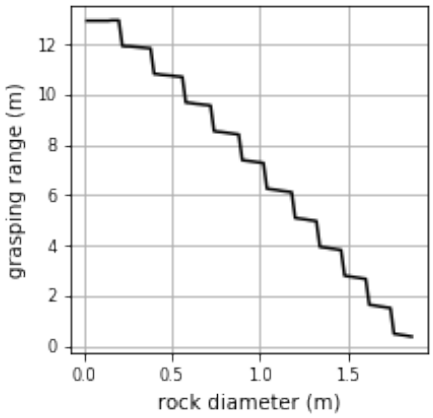

Figure 8. Resultant manipulation capabilities

5. CONCLUSION

This paper sets out the need for a general purpose gripper capable of autonomously collecting objects from a rough terrain in microgravity. It shows the limitations of current methodology and proposes a new modular reconfigurable concept to address them.

The kinematics support a large range of target scales with a common design and control methodology. By combining the end effector with the manipulator arm, the robot is very efficient in the range of targets it can handle; it is able to trade target diameter for additional reach.

A detailed dynamical model is needed to quantify and predict the disturbances caused to the base station by arm motion, as the base may not immovably attached to the surface. The concept would appear to allow a great variety of sizes of target to be manipulated with a single robot and early results are promising. Control schemes and pathfinding will also need validation. SSSB surface distribution data will need to be combined with SNUG modelling to determine the optimal return for a given mass budget.

6. ACKNOWLEDGEMENT

This study is supported by the Engineering and Physical Science Research Council (EPSRC), UK and Airbus Defence and Space, UK.

REFERENCES

[1] P. T. Metzger, A. Muscatello, R. P. Mueller, and J. Mantovani. Affordable, rapid bootstrapping of the space industry and solar system civilization. *J. of Aerospace Eng.*, 26(1):18–29, 2012.

[2] K. Skonieczny, D. S. Wettergreen, and W. R. Whittaker. Advantages of continuous excavation

in lightweight planetary robotic operations. *Sci.*, 35(9):1121 – 1139, 2016.

[3] D. Latimer. Excavation in space: A survey of automation technologies. In *Proc. of the 2001 Space Studies Inst. Conf.*, May 2001.

[4] R. Mueller and P. Van Susante. A rev. of lunar regolith excavation robotic device prototypes. In *AIAA SPACE 2011 Conf. & Exposition*, page 7234, Long Beach, USA, 2011.

[5] R. P. Mueller, R. E. Cox, T. Ebert, J. D. Smith, and J. M. Schuler. Regolith Advanced Surface Systems Operations Robot (RASSOR). In *2013 IEEE Aerospace Conf.*, Big Sky, USA, May 2013.

[6] A. Ellery, P. Lowing, P. Wanjara, M. Kirby, I. Mellor, and G. Doughty. Ffc cambridge process with metal 3d printing as universal in-situ resource utilisation. In *Advanced Space Technol. Robotics and Automation (ASTRA) Conf.*, 2017.

[7] IAU resolution B5: "definition of a planet in the solar system". `https://www.iau.org/administration/resolutions/general_assemblies/`, 2006.

[8] NASA JPL Center for Near Earth Object Studies. Discovery statistics. `https://cneos.jpl.nasa.gov/stats/size.html`, 2019 (accessed April 22, 2019).

[9] A. F. Cheng. Near earth asteroid rendezvous: mission summary. *Asteroids III*, 1:351–366, 2002.

[10] J. Saito, H. Miyamoto, R. Nakamura, M. Ishiguro, Michikami, A.M. T. Nakamura, et al. Detailed images of asteroid 25143 itokawa from hayabusa. *Sci.*, 312(5778):1341–1344, 2006.

[11] S. Ulamec, C. Fantinati, M. Maibaum, K. Geurts, J. Biele, S. Jansen, O. Küchemann, B. Cozzoni, F. Finke, V. Lommatsch, et al. Rosetta lander–landing and operations on comet 67p/churyumov–gerasimenko. *Acta Astronautica*, 125:80–91, 2016.

[12] H. Sawada, R. Okazaki, S. Tachibana, K. Sakamoto, Y. Takano, C. Okamoto, et al. Hayabusa2 sampler: Collection of asteroidal surface material. *Space Sci. Rev.*, 208(1):81–106, Jul 2017.

[13] B. Rizk, C. Drouet d'Aubigny, D. Golish, C. Fellows, C. Merrill, P. Smith, et al. Ocams: The osiris-rex camera suite. *Space Sci. Rev.*, 214(1):26, Jan 2018.

[14] K. Zacny, E. B. Bierhaus, D. T. Britt, B. Clark, C. M. Hartzell, L. Gertsch, A. V. Kulchitsky, J. B. Johnson, P. Metzger, D. M. Reeves, et al. Geotechnical properties of asteroids affecting surface operations, mining, and in situ resource utilization activities. In *Primitive Meteorites and Asteroids*, pages 439–476. Elsevier, 2018.

[15] N. Murdoch, P. Sánchez, S. R. Schwartz, and H. Miyamoto. Asteroid surface geophysics. *Asteroids IV*, pages 767–792, 2015.

[16] C. W. Hergenrother, M. A. Barucci, O. Barnouin, B. Bierhaus, Binzel, et al. The design reference asteroid for the osiris-rex mission target (101955) bennu. *arXiv preprint arXiv:1409.4704*, 2014.

[17] A. Hérique, B. Agnus, E. Asphaug, A. Barucci, P. Beck, Bellerose, et al. Direct observations of asteroid interior and regolith structure: Sci. measurement requirements. *Advances in Space Res.*, 62(8):2141–2162, 2018.

[18] E. B. Bierhaus, B. C. Clark, J. W. Harris, K. S. Payne, R. D. Dubisher, D. W. Wurts, et al. The osiris-rex spacecraft and the touch-and-go sample acquisition mechanism (tagsam). *Space Sci. Rev.*, 214(7):107, Sep 2018.

[19] JAXA. The touchdown site. `http://www.hayabusa2.jaxa.jp/en/topics/20190220e_TDPoint/`, 2019 (accessed April 22, 2019).

[20] D. D. Mazanek, R. G. Merrill, S. P. Belbin, D. M. Reeves, B. J. Naasz, P. A. Abell, and K. Earle. Asteroid redirect robotic mission: Robotic boulder capture option overview. In *AIAA SPACE 2014 Conf. and Exposition*, page 4432, 2014.

[21] J. L. Forshaw, G. S. Aglietti, N. Navarathinam, H. Kadhem, T. Salmon, A. Pisseloup, E. Joffre, T. Chabot, I. Retat, R. Axthelm, et al. Removedebris: An in-orbit active debris removal demonstration mission. *Acta Astronautica*, 127:448–463, 2016.

[22] L. Cercós, R. Stefanescu, A. Medina, R. Benvenuto, M. Lavagna, I. González, N. Rodríguez, K. Wormnes, et al. Validation of a net active debris removal simulator within parabolic flight experiment. In *12th Int. Symp. on Artificial Intelligence, Robotics and Automation in Space, Montreal, Canada*, pages 17–19, 2014.

[23] S. Makita and W. Wan. A survey of robotic caging and its applications. *Advanced Robotics*, 31(19-20):1071–1085, 2017.

[24] W. Wan, R. Fukui, M. Shimosaka, T. Sato, and Y. Kuniyoshi. Grasping by caging: A promising tool to deal with uncertainty. In *2012 IEEE Int. Conf. Robotics and Automation*, pages 5142–5149, St Paul,USA, May 2012.

[25] M. Yim, K. Roufas, D. Duff, Y. Zhang, C. Eldershaw, and S. Homans. Modular Reconfigurable Robots in Space Applications. *Sci.*, 14:225 – 237, 2003.

[26] R. Marc, M. Ruciński, A. Coates, E. Allouis, M. Garland, D. Lachat, A. Donchev, W. Tubby, J. Hampton, A. Kisdi, et al. Design concepts and implementation of the lightweight advanced robotic arm demonstrator (larad). In *Proc. of the 67th Int. Astronautical Congress (IAC), Guadalajara, Mexico*, pages 26–30, Guadalajara, Mexico, May 2016.

[27] P. Callen. Robotic transfer and interfaces for external iss payloads. In *3rd Annual ISS Res. and Develop. Conf.*, Chicago USA, June 2014.

[28] J. Shintake, S. Rosset, B. Schubert, D. Floreano, and H. Shea. Versatile soft grippers with intrinsic electroadhesion based on multifunctional polymer actuators. *Advanced Materials*, 28(2):231–238, 2016.